Gravitational waves from remnant massive neutron stars of binary neutron star merger: Viscous hydrodynamics effects

Masaru Shibata and Kenta Kiuchi

Center of Gravitational Physics, Yukawa Institute for Theoretical Physics, Kyoto University, Kyoto 606-8502, Japan

Employing a simplified version of the Israel-Stewart formalism of general-relativistic shear-viscous hydrodynamics, we explore the evolution of a remnant massive neutron star of binary neutron star merger and pay special attention to the resulting gravitational waveforms. We find that for the plausible values of the so-called viscous alpha parameter of the order 10^{-2} the degree of the differential rotation in the remnant massive neutron star is significantly reduced in the viscous time scale, $\lesssim 5$ ms. Associated with this, the degree of nonaxisymmetric deformation is also reduced quickly, and as a consequence, the amplitude of quasiperiodic gravitational waves emitted also decays in the viscous time scale. Our results indicate that for modeling the evolution of the merger remnants of binary neutron stars we would have to take into account magnetohydrodynamics effects, which in nature could provide the viscous effects.

I. INTRODUCTION

The merger of binary neutron stars is one of the promising sources of gravitational waves for ground-based gravitational-wave detectors such as advanced LIGO, advanced VIRGO, and KAGRA [1]. This fact has motivated the community of numerical relativity to construct a reliable model for the inspiral, merger, and postmerger stages of binary neutron stars by numerical-relativity simulations.

The recent discoveries of two-solar mass neutron stars [2] strongly constrain the possible evolution processes in the merger and postmerger stages because the presence of these heavy neutron stars implies that the equation of state of neutron stars has to be stiff enough to support the self-gravity of the neutron stars with mass $\gtrsim 2\,M_\odot$. Numerical-relativity simulations with a variety of hypothetical equations of state that can reproduce the two-solar-mass neutron stars have shown that massive neutron stars surrounded by a massive torus are likely to be the canonical remnants formed after the merger of binary neutron stars of typical total mass 2.6–2.7 $M_\odot$ (see, e.g., Refs. [3–8] and Refs. [9,10] for a review).

Because the remnant massive neutron stars are rapidly rotating and have a nonaxisymmetric structure, they could be a strong emitter of high-frequency gravitational waves of frequency 2.0–3.5 kHz (e.g., Refs. [5–10]). This aspect has attracted special attention in the last decade, and many *purely* hydrodynamics or radiation hydrodynamics simulations have been performed in numerical relativity for predicting the gravitational waveforms. However, the remnant massive neutron stars and a torus surrounding them should be strongly magnetized because during the merger process the Kelvin-Helmholtz instability inevitably occurs and contributes to significantly enhancing the magnetic-field strength in a time scale much shorter than

the dynamical one, $\lesssim 1$ ms [11,12]. In addition, the remnant massive neutron stars are in general differentially rotating, and hence the magnetic field may be further amplified through magnetorotational instability [13]. As a result of these instabilities, magnetohydrodynamics (MHD) turbulence shall develop as shown by a number of high-resolution MHD simulations for accretion disks (see, e.g., Refs. [14–16]), and it is likely to determine the evolution of the system in the following manner: (i) angular momentum would be quickly redistributed; (ii) the degree of the differential rotation would be quickly reduced; and (iii) as a consequence of the evolution of the rotational velocity profile, nonaxisymmetric deformation may be modified. By these effects, the remnant massive neutron stars may result in a weak emitter of high-frequency gravitational waves.

For rigorously exploring these processes resulting from a turbulence state, extremely-high-resolution MHD simulation is necessary (see, e.g., Ref. [12] for an effort on this). However, such simulations will not be practically feasible at least in the next several years because of the limitation of the computational resources. One phenomenological approach for exploring the evolution of the system that is subject to angular-momentum transport is to employ viscous hydrodynamics in general relativity [17–19]. The viscosity is likely to be induced effectively by the local MHD turbulence [14–16], and thus relying on viscous hydrodynamics implies that local MHD and turbulence processes are coarse grained and effectively taken into account. The merit in this approach is that we do not have to perform an extremely-high-resolution simulation and we can save the computational costs significantly.

In this paper, we perform a viscous hydrodynamics simulation for a remnant massive neutron star of binary neutron star merger. Following our previous work [19],

123003-1

we employ the Israel-Stewart-type formalism [20], in which the resulting viscous hydrodynamics equations are not parabolic type but telegraph type and, hence, the causality is preserved [21], by contrast to the cases in which Navier-Stokes-type equations [22] are employed. In Ref. [19], we show that with our choice of the viscous hydrodynamics formalism, it is feasible to perform long-term stable simulations for strongly self-gravitating systems.

This paper is organized as follows. In Sec. II, we briefly review our formulation for shear-viscous hydrodynamics. After we briefly describe our setting for numerical simulations in Sec. III, we present the results of viscous hydrodynamics evolution for the remnant of binary neutron star merger in Sec. IV. Section V is devoted to a summary. Throughout this paper, c denotes the speed of light.

II. FORMULATION FOR VISCOUS HYDRODYNAMICS

A. Basic equations

We write the stress-energy tensor of a viscous fluid as [19]

$$T_{ab} = \rho h u_a u_b + P g_{ab} - \rho h c^{-2} \nu \tau^0_{ab}, \qquad (2.1)$$

where ρ is the rest-mass density, h is the specific enthalpy, u^a is the 4-velocity, P is the pressure, g_{ab} is the spacetime metric, ν is the viscous coefficient for the shear stress, and τ^0_{ab} is the viscous tensor. Here, ρ obeys the continuity equation $\nabla_a(\rho u^a) = 0$. In terms of the specific energy ε and pressure P, h is written as $h = c^2 + \varepsilon + P/\rho$. τ^0_{ab} is the symmetric tensor and satisfies $\tau^0_{ab} u^a = 0$. We suppose that ν is a function of ρ, ε, P, and angular velocity Ω and will give the relation below.

Taking into account the prescription of Ref. [20], we define that τ^0_{ab} obeys the evolution equation

$$\mathcal{L}_u \tau^0_{ab} = -\zeta(\tau^0_{ab} - \sigma_{ab}), \qquad (2.2)$$

where $\mathcal{L}_u$ denotes the Lie derivative with respect to u^a and we write σ_{ab} as

$$\sigma_{ab} := h_a{}^c h_b{}^d (\nabla_c u_d + \nabla_d u_c) = \mathcal{L}_u h_{ab}, \qquad (2.3)$$

with $h_{ab} = g_{ab} + u_a u_b$ and ∇_a the covariant derivative associated with g_{ab}. ζ is a constant of the (time)$^{-1}$ dimension, which has to be chosen in an appropriate manner so that τ^0_{ab} approaches σ_{ab} in a short time scale: we typically choose it so that ζ^{-1} is shorter than the dynamical time scale of given systems (but it should be much longer than the time-step interval of numerical simulations, Δt).

Equation (2.3) can be rewritten as

$$\mathcal{L}_u \tau_{ab} = -\zeta \tau^0_{ab}, \qquad (2.4)$$

where $\tau_{ab} := \tau^0_{ab} - \zeta h_{ab}$. We employ this equation for τ_{ab} as one of the basic equations of viscous hydrodynamics, and hence the stress-energy tensor is rewritten as follows:

$$T_{ab} = \rho h(1 - c^{-2}\nu\zeta)u_a u_b + (P - \rho h c^{-2}\nu\zeta)g_{ab} - \rho h c^{-2}\nu\tau_{ab}. \qquad (2.5)$$

Then, the viscous hydrodynamics equations are derived from $\nabla_a T^a{}_b = 0$ (see Ref. [19] for details).

B. Setting viscous parameter

In the so-called α-viscous model, ν is written as (see, e.g., Ref. [23])

$$\nu = \alpha_v c_s^2 \Omega^{-1}, \qquad (2.6)$$

where c_s is the sound velocity and Ω denotes the typical value of the angular velocity. α_v is the so-called α-viscous parameter, which is a dimensionless constant supposed to be of the order 10^{-2} or more as suggested by latest high-resolution MHD simulations for accretion disks [14–16].

In this paper, we consider viscous hydrodynamics evolution of a weakly differentially rotating neutron star, and hence we set

$$\nu = \alpha_v c_s^2 \Omega_f^{-1}, \qquad (2.7)$$

where we set $\Omega_f = 2\pi/(0.5\ \mathrm{ms})$ which is close to the maximum value of the angular velocity for the initial state of remnant massive neutron stars (see, e.g., Fig. 2). We note that $c_s \Omega_f^{-1} \lesssim 15$ km with this setting in our present model. Since $c_s \Omega_f^{-1}$ should not exceed the size of the neutron star, this is a reasonable setting.

The viscous angular momentum transport time scale is approximately defined by R^2/ν and estimated to be

$$t_{\mathrm{vis}} \approx 4.4\ \mathrm{ms}\left(\frac{\alpha_v}{0.01}\right)^{-1}\left(\frac{c_s}{0.5c}\right)^{-2}\left(\frac{R}{10\ \mathrm{km}}\right)^2$$

$$\times \left(\frac{\Omega}{10^4\ \mathrm{rad/s}}\right), \qquad (2.8)$$

where we assumed Eq. (2.6) for ν. We note that for the central region of the merger remnant the sound velocity is quite high, typically as $c_s \sim 0.5c$ with maximum $\sim 0.6c$ (and hence the velocity in most of the region of the merger remnant is subsonic). In the vicinity of the rotation axis (for a small value of R), the time scale may be even shorter. Thus, within $\sim 5(\alpha_v/0.01)^{-1}$ ms, the angular momentum is expected to be redistributed in the merger remnant. In the following, we will show that this is indeed the case.

III. SETTING FOR NUMERICAL SIMULATIONS

A. Brief summary of simulation setting

For solving Einstein's evolution equation, we employ the original version of Baumgarte-Shapiro-Shibata-Nakamura formulation with a puncture gauge [24]. The gravitational-field equations are solved in the usual fourth-order finite differencing scheme (e.g., Ref. [9] for a review).

The initial condition of the present simulations is imported from a simulation result for binary neutron star mergers. That is, we first performed a purely hydrodynamics simulation for the merger up to ∼5 ms after the onset of the merger. The merger simulation was performed with a grid resolution, which is the same as in the high-resolution viscous hydrodynamics simulation (see below). Then, we extract the weighted rest-mass density, $\rho_* := \rho \alpha u^t \psi^6$; weighted spatial velocity field, $\hat{u}_i := h u_i$; and specific energy, $e := h \alpha u^t - P/(\rho \alpha u^t)$, where α is the lapse function and ψ is the conformal factor for the three-dimensional metric, $\psi = [\det(\gamma_{ij})]^{1/12}$, with γ_{ij} the three-dimensional metric. We prepare these quantities in a new computational domain for viscous hydrodynamics and then solve initial value equations (constraint equations) assuming the conformal flatness of the system. If necessary, an interpolation for data is performed (this is the case for lower-resolution runs). The assumption of the conformal flatness is acceptable because the magnitude for all the components of $\psi^{-4}\gamma_{ij} - \delta_{ij}$ is much smaller than unity (at most 0.02) for the merger remnant employed in this paper. For the initial condition, we set $\tau_{ab}^0 = 0$ for simplicity.

In this study, we employ the so-called H4 equation of state [25], approximating it by a piecewise polytropic equation of state with four pieces [26]. During the numerical evolution, we employ a modified version of the piecewise polytropic equation of state in the form

$$P = P_{\text{pwp}}(\rho) + (\Gamma - 1)\rho[\varepsilon - \varepsilon_{\text{pwp}}(\rho)], \qquad (3.1)$$

where $\varepsilon_{\text{pwp}}(\rho)$ denotes the specific internal energy associated with P_{pwp} satisfying $d\varepsilon_{\text{pwp}} = -P_{\text{pwp}}d\rho^{-1}$ and the adiabatic constant Γ is set to be 1.8. Key quantities for the initial data employed in this work are shown in Table I.

TABLE I. Key quantities for the initial condition employed in the present viscous hydrodynamics simulations: baryon rest mass M_*, gravitational mass M, maximum rest-mass density $\rho_{\max}$, angular velocity at $R = 0$, Ω_a, maximum angular velocity $\Omega_{\max}$, and dimensionless angular momentum J/M^2. The mass, density, and angular velocity are shown in units of $M_\odot$, g/cm³, and rad/s, respectively.

M_*	M	$\rho_{\max}$	Ω_a	$\Omega_{\max}$	J/M^2
2.94	2.62	1.0×10^{15}	3.2×10^3	9.4×10^3	0.76

Numerical simulations are performed in Cartesian coordinates (x, y, z) with a nonuniform grid. Specifically, we employ the grid structure (the same profile is chosen for y and z)

$$\Delta x = \begin{cases} \Delta x_0 & |x| \le x_{\text{in}}, \\ \Delta x_i = f \Delta x_{i-1} & |x| > x_{\text{in}}, \end{cases} \qquad (3.2)$$

where Δx_0 is the grid spacing in an inner region with $x_{\text{in}} \approx 22.5$ km. $\Delta x_i := x_{i+1} - x_i$ with x_i the location of the ith grid. At $i = \text{in}$, $\Delta x_i = \Delta x_0$. f determines the nonuniform degree of the grid spacing, and we set it to be 1.03. We change Δx_0 as 295 m (low resolution), 220 m (middle resolution), and 148 m (high resolution) to confirm that the dependence of the numerical results on the grid resolution is weak (see Appendix A). The outer boundary is located at $\approx \pm 2100$ km along each axis for all the grid resolutions. Unless otherwise stated, we will show the results in the high-resolution runs in the following. We note that the wavelength of gravitational waves emitted by remnants of binary neutron star mergers is typically 120 km in our present model. Thus, with this setting of the computational domain, the outer boundary is located in a wave zone. To suppress the growth of unstable modes associated with the high-frequency numerical noises, we incorporate a six-order Kreiss-Oliger-type dissipation term as in our previous study [19].

The viscous coefficient is written in the form of Eq. (2.7). Latest high-resolution MHD simulations for accretion disks [14–16] have suggested that the α-viscous parameter would be of the order 10^{-2} or more. Taking into account this numerical-experimental fact, we choose $\alpha_v = 0.01$ and 0.02. ζ is set to be $\approx 2\Omega_{\max} \approx 6\Omega_a$ in this work.

IV. NUMERICAL RESULTS

Figures 1 and 2 display the evolution of the profiles for the rest-mass density and angular velocity on the equatorial plane, respectively. For calculating the angular velocity, we first determine the center of mass (x_0, y_0) of the massive neutron star on the equatorial plane. Here, x_0 and y_0 are in general slightly different from zero. Then, the angular velocity is defined by $\Omega = [-(y - y_0)v^x + (x - x_0)v^y]/R^2$ where $R = \sqrt{(x - x_0)^2 + (y - y_0)^2}$. For these figures, the left, middle, and right columns show the results for $\alpha_v = 0$, 0.01, and 0.02, respectively. The top, middle, and bottom rows show the results for $t \approx 0$, 3, and 21 ms, respectively.

As we have always observed in the merger simulations [4–10], the remnants of binary neutron star mergers have a nonaxisymmetric structure. In the absence of viscous effects, this nonaxisymmetric structure is preserved for the time scale of >10 ms (see the left column of Fig. 1) because of the absence of efficient processes of angular momentum transport, and thus the differential rotation is preserved (see the left column of Fig. 2). Note that the
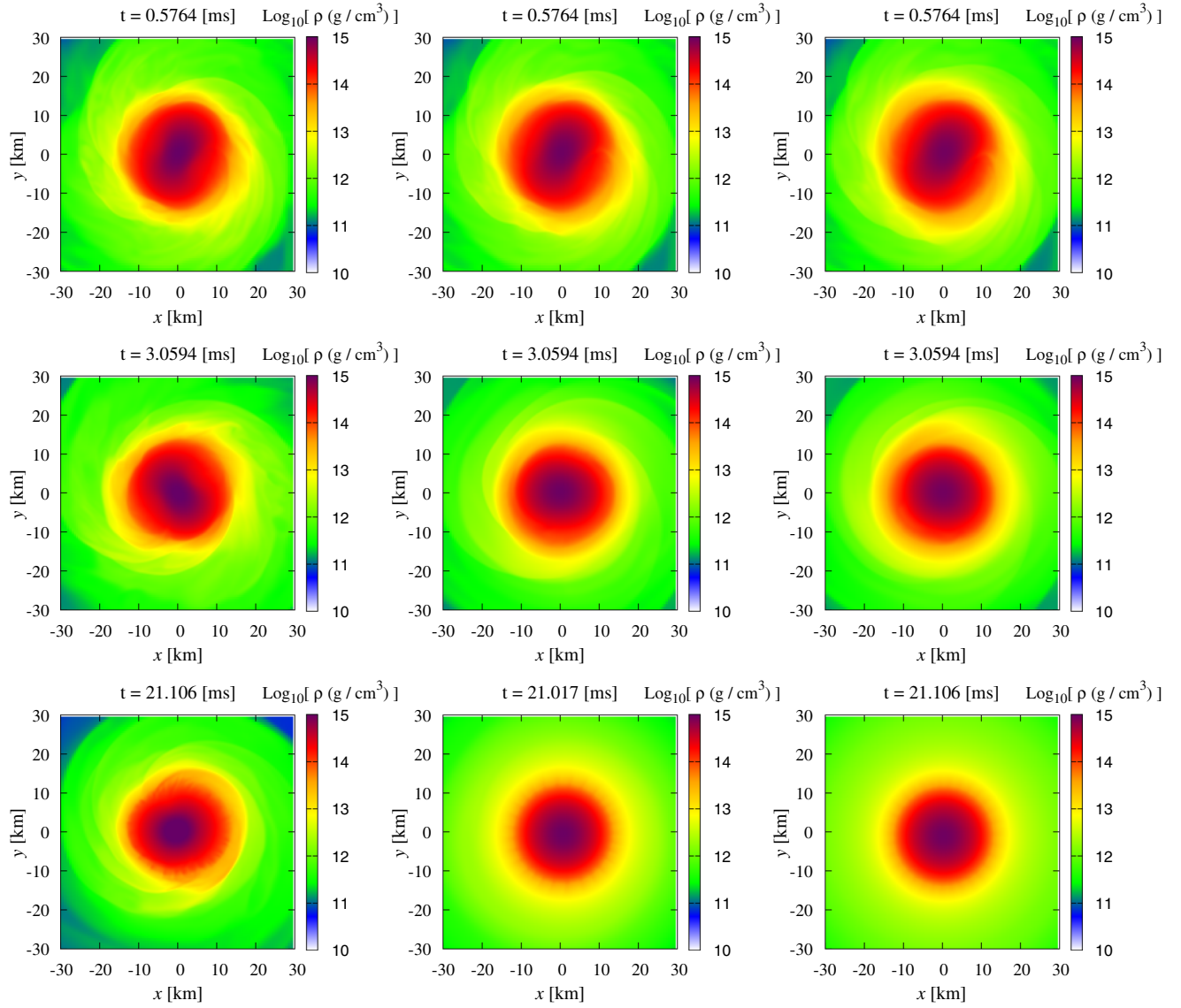
FIG. 1.   Evolution of rest-mass density profiles on the equatorial plane with $\alpha_v = 0$ (left column), 0.01 (middle column), and 0.02 (right column). Each column shows three snapshots of different time: the top, middle, and bottom rows show the results for $t \approx 0$, 3, and 21 ms, respectively.

torque exerted by the massive neutron star of nonaxisymmetric structure to surrounding material transports angular momentum outward, but its time scale is not as short as 10 ms.

By contrast, in the presence of viscosity with $\alpha_v = O(10^{-2})$, the angular momentum transport process works efficiently. The middle and right columns of Fig. 2 illustrate that the angular velocity profile is modified approximately to a uniform profile for $R < 15$ km in the time scale of less than 10 ms. As a result, the rest-mass density profile is also modified quickly. The middle and right columns of Fig. 1 illustrate that in a time scale of $\ll 20$ ms the nonaxisymmetric structure disappears and the remnant becomes approximately axisymmetric.

The disappearance of the nonaxisymmetric structure is reflected in the fact that spiral arms in the envelope disappear for $\alpha_v = 0.01$ and 0.02 (by contrast, for $\alpha_v = 0$, the spiral arms are continuously observed). This results from the viscous effect by which torque exerted by the remnant massive neutron star is significantly weakened due to the reduced degree of the nonaxisymmetry. It is also found from Fig. 1 that in the presence of nonzero viscosity the matter expands outward: for $\alpha_v = 0$, the region with $\rho \geq 10^{12}$ g/cm^3 is extended only to $R \sim 20$ km, but for $\alpha_v = 0.01$ and 0.02, it is extended to $R \sim 30$ km.

Figure 3 shows the evolution of the averaged angular velocity along the cylindrical radius R. The averaged angular velocity is obtained by averaging Ω along the
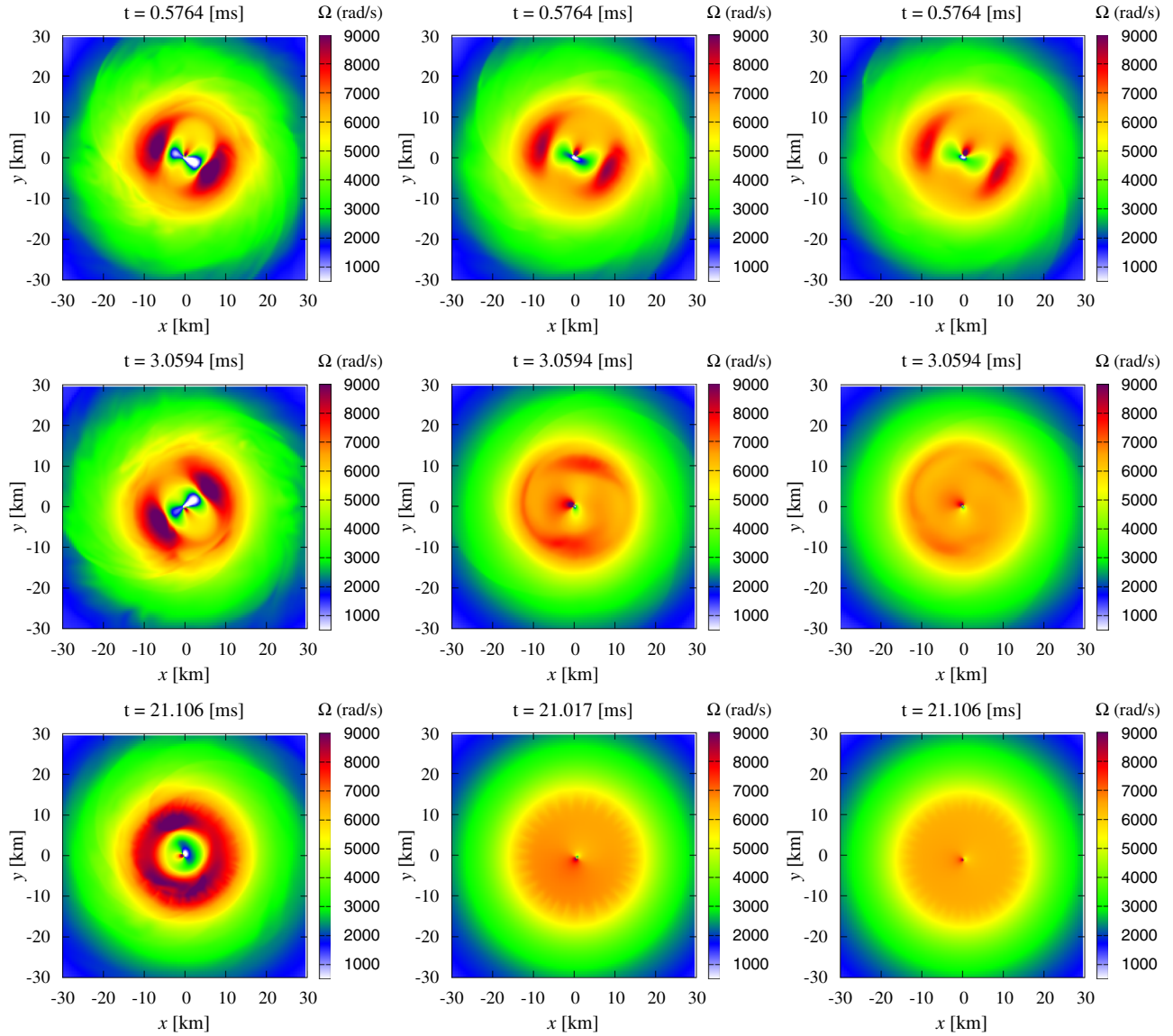
FIG. 2. The same as Fig. 1 but for the angular velocity. The angular velocity is determined by $[-(y - y_0)v^x + (x - x_0)v^y]/$ $[(x - x_0)^2 + (y - y_0)^2]$ where (x_0, y_0) is a mass center appropriately determined: x_0 and y_0 are slightly different from zero. Note that for the white region [near (x_0, y_0)] we cannot accurately determine the angular velocity.
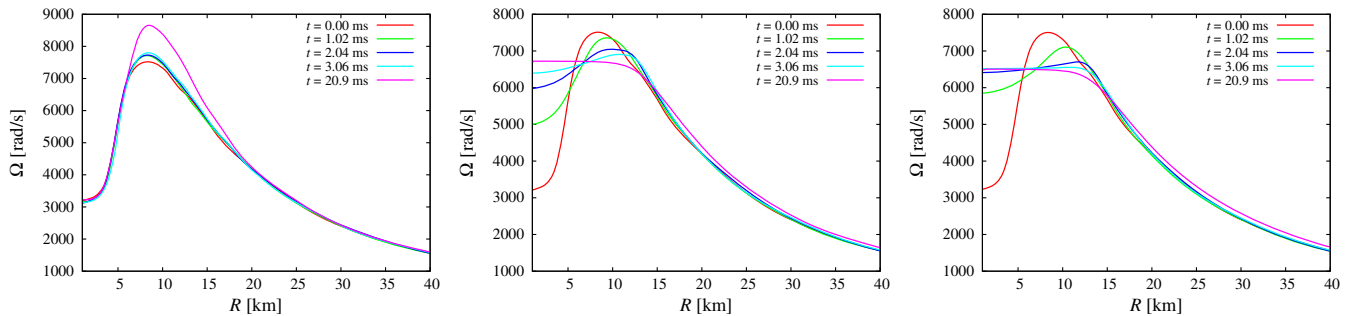

FIG. 3. Averaged angular-velocity profiles along the cylindrical radius at selected time slices for the models with $\alpha_v = 0$ (left column), 0.01 (middle column), and 0.02 (right column).
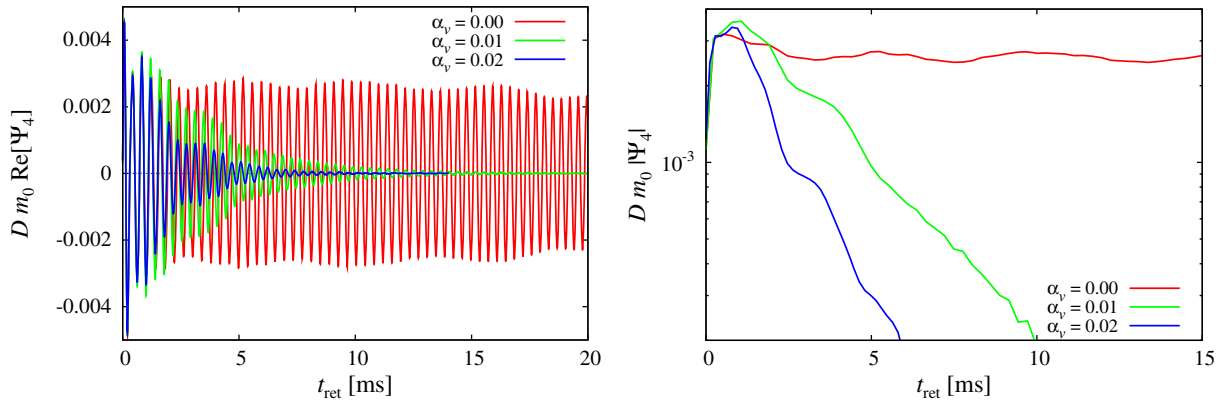
FIG. 4.   Left: gravitational waveforms for $\alpha_v = 0$, 0.01, and 0.02. Here, we plot the real part of Ψ_4 for the $l = m = 2$ spin-weighted spherical-harmonics component. D and $m_0 (= 2.7\ M_\odot)$ are the distance from the source to the observer and initial gravitational mass of the binary system. We assume that the observer of gravitational waves is located along the rotation axis of the massive neutron star. Right: evolution of the absolute value of Ψ_4. To clarify the exponential damping of the curves, for plotting the right panel, we apply a filter to $|\Psi_4|$ in order to erase high-frequency noises.

azimuthal angle $\varphi = \tan^{-1}[(y - y_0)/(x - x_0)]$ for fixed values of R and z as

$$\bar{\Omega}(R, z) = \frac{1}{2\pi} \int_0^{2\pi} \Omega(R, z, \varphi) d\varphi. \qquad (4.1)$$

As is often observed in numerical-relativity simulations (e.g., Ref. [3]), the merger remnants are initially differentially rotating, and the maximum of the angular velocity Ω is located in the vicinity of the stellar surface of the remnant massive neutron stars. Such profiles are formed during the merger process, because at the onset of the merger, two neutron stars with opposite velocity vectors collide with each other, and kinetic energy is dissipated at their contact surfaces. In the absence of the viscous effects, this profile is preserved for a time scale longer than 20 ms. By contrast, in the presence of the viscous effects, this differential rotation disappears in the viscous time scale t_{vis} because of the efficient viscous angular momentum transport. Because the peak of Ω is initially located near the stellar surface, the angular velocity near the rotation axis is increased. That is, the angular momentum is transported inward inside the massive neutron star. In this example, the rotation period of the resulting massive neutron star, $2\pi/\Omega$, is relaxed uniformly to be ≈ 1 ms.

Associated with the viscous angular momentum transport, a massive torus surrounding the central massive neutron star develops in the presence of viscosity. The rest mass of the torus, measured for the matter with $R \geq 10$ and 15 km at $t = 20$ ms, is ≈ 0.41 and $0.19\ M_\odot$ for $\alpha_v = 0.02$ and ≈ 0.38 and $0.17\ M_\odot$ for $\alpha_v = 0.01$. The torus mass for $\alpha_v = 0$ at $t = 20$ ms is ≈ 0.26 and $0.15\ M_\odot$ for $R \geq 10$ and 15 km, and hence the viscous angular momentum transport enhances the massive torus formation.

As shown in Fig. 3, the torus is preserved to be differentially rotating around the central massive neutron star, and hence it is still subject to viscous heating and viscous angular momentum transport. As indicated in our previous study [19], the inner part of the torus will be heated up significantly due to the long-term viscous heating, and eventually an outflow could be driven with a substantial amount of mass ejection. Exploring the generation processes of the outflow and mass ejection by a long-term numerical-relativity simulation is one of our future issues.

These viscous effects are reflected intensely in gravitational waves emitted by the remnant massive neutron star. Figure 4 shows the gravitational waveforms for $\alpha_v = 0$, 0.01, and 0.02 altogether. Here, we plot the real part of the outgoing components of the complex Weyl scalar (the so-called Ψ_4) for the $l = m = 2$ spin-weighted spherical-harmonics component. For $\alpha_v = 0$, quasiperiodic gravitational waves are emitted for a time scale much longer than 10 ms, reflecting the fact that the nonaxisymmetric structure of the massive neutron star is preserved (this waveform is essentially the same as what we found in our merger simulation [6]). The right panel of Fig. 4 clearly shows that the amplitude of gravitational waves is nearly constant for this case. By contrast, the gravitational-wave amplitude decreases exponentially in time in the viscous time scale for $\alpha_v \neq 0$. This reflects the fact that the nonaxisymmetric structure of the massive neutron star disappears in the viscous time scale. This suggests that in the presence of MHD turbulence which would induce turbulence viscosity the merger remnant of binary neutron stars may not emit high-amplitude gravitational waves for a time scale longer than ~ 10 ms.

The right panel of Fig. 4 shows that the amplitude of gravitational waves damps in an exponential manner $\propto \exp(-t/\tau)$ where τ is the e-folding damping time scale. In the present results, τ is approximately written as
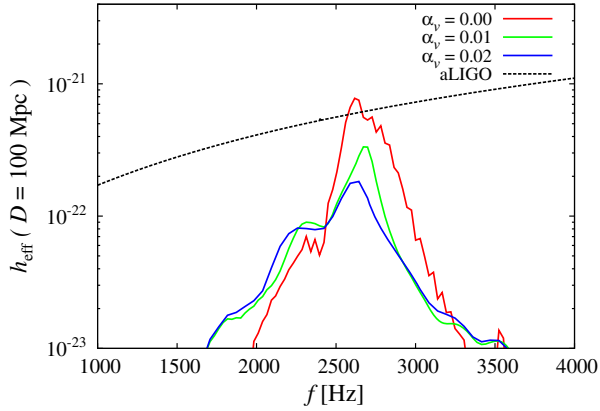
FIG. 5.   The spectrum of gravitational waves for $\alpha_v = 0$, 0.01, and 0.02 with $D = 100$ Mpc. We assume that the observer is located along the most optimistic direction (i.e., along the rotation axis). The spectrum, $h_{\rm eff}$, is defined by $|\tilde{h}(f)f|$ where $\tilde{h}(f)$ is the Fourier spectrum of gravitational waves. The dashed curve referred to as aLIGO denotes $[S_n(f)f]^{1/2}$, where S_n is the one-sided noise spectrum density for the "Zero Detuning High Power" configuration of advanced LIGO [27].

$$\tau \approx 3.6 \text{ ms} \left(\frac{\alpha_v}{0.01}\right)^{-1}. \qquad (4.2)$$

This time scale agrees approximately with the time scale for the change of the angular velocity profiles found in Fig. 3.

We note that the author of Ref. [18] recently performed a viscous hydrodynamics simulation for the merger of binary neutron stars. He also showed that the luminosity of gravitational waves decreases with the increase of the viscous coefficient, although he focused only on the case with a small viscous parameter [in the terminology of alpha viscosity, he focuses only on the cases of $\alpha_v = O(10^{-3})$ or less].

Figure 5 plots the spectrum of gravitational waveforms defined by $h_{\rm eff} := |f\tilde{h}(f)|$ where $\tilde{h}(f)$ is the Fourier transformation of gravitational waves defined by

$$\tilde{h}(f) := \int_0^T h(t)e^{-2\pi ift}dt. \qquad (4.3)$$

Here, T corresponds to the final time of the simulation, and $h(t) = h_+ - ih_\times$ with h_+ and $h_\times$ denoting the plus and cross modes of gravitational waves. In numerical simulation, we obtain $\ddot{h}(t)(= \Psi_4)$, and hence we calculate $\tilde{h}(f)$ by

$$\tilde{h}(f) = -\int_0^T \frac{\Psi_4(t)}{(2\pi f)^2} e^{-2\pi ift}dt. \qquad (4.4)$$

Figure 5 shows that the peak amplitude decreases monotonically with the increase of α_v, while the peak

frequency depends only weakly on the value of α_v. We note that we stopped our simulations at $t \approx 25$ ms, and hence for $\alpha_v = 0$ for which gravitational waves are emitted for a time scale longer than 25 ms, the peak amplitude of $\tilde{h}(f)$ would be underestimated.

To qualitatively understand the behavior on the decrease of the peak amplitude for the spectrum, we consider a simple model in which the gravitational waveforms denoted by $h := h_+ - ih_\times$ are written as a monochromatic form $A \exp(2\pi if_p t - t/\tau_v)$ where A is the amplitude of h, f_p is the monochromatic frequency of gravitational waves, and τ_v denotes the damping time of the gravitational-wave amplitude [which should be proportional to α_v^{-1} and approximately equal to τ in Eq. (4.2)]. Then, at the peak of the Fourier spectrum, $f = f_p$, we obtain

$$|\tilde{h}(f_p)| = [1 - \exp(-T/\tau_v)]A\tau_v. \qquad (4.5)$$

Thus, for $T/\tau_v \gg 1$, $|\tilde{h}(f_p)| = A\tau_v$. Since $|\tilde{h}(f_p)| = AT$ for $\tau_v \to 0$, the peak amplitude is by a factor of τ_v/T (i.e., by a factor of several) smaller than that in the nonviscous case. The numerical results agree qualitatively with this rule.

V. SUMMARY

Employing a simplified formalism for general-relativistic viscous hydrodynamics that can minimally capture the effects of the shear-viscous stress, we performed numerical-relativity simulations for the evolution of a remnant of binary neutron star merger, paying particular attention to gravitational waves emitted by the merger remnant. As often found in the purely hydrodynamical simulations [3–10], in the absence of viscous effects, the merger remnant emits quasiperiodic gravitational waves for a time scale longer than 10 ms, keeping their amplitude high and their frequency approximately constant. However, in the presence of viscous effects, the amplitude of gravitational waves damps in an exponential manner in time. The time scale of the exponential damping agrees approximately with the viscous time scale, which is $\lesssim 5$ ms for a plausible viscous coefficient with $\alpha_v \gtrsim 0.01$. This suggests that the merger remnant of binary neutron stars may not be a strong emitter of gravitational waves.

In reality, the viscous effects would be induced by MHD turbulence. Since we do not know whether the MHD turbulence is equivalent to the shear viscous-hydrodynamical turbulence, our present result is still speculative. To obtain the true answer in this problem, we have to perform an extremely-high-resolution MHD simulation in the future. However, it will not be an easy task to perform such simulations in the near future because of the limitation of computational resources. Thus, the best attitude we can currently take is to keep in mind that there would be a variety of the possibilities for the evolution of the merger
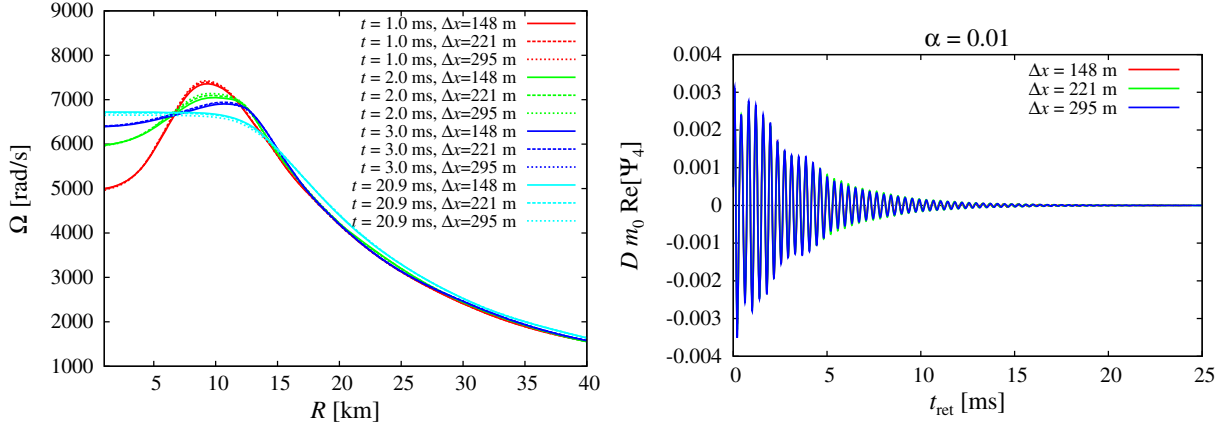
FIG. 6.   Left: the averaged angular velocity along the cylindrical radius at selected time slices for three different grid resolutions. Right: the gravitational waveforms for $\alpha_v = 0.01$ with three different grid resolutions.
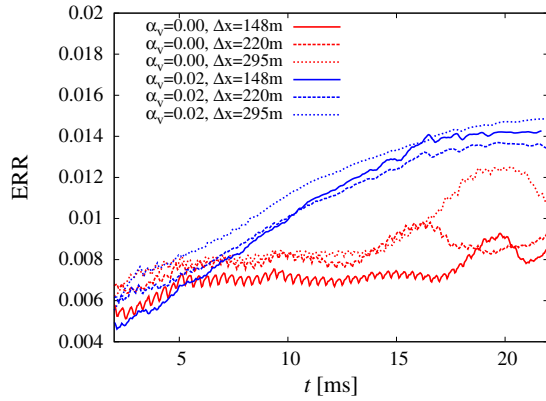

FIG. 7.   Evolution for the violation of the Hamiltonian constraint [ERR defined in Eq. (A1)].

remnants of binary neutron stars because we have not yet fully understood the physics for the merger remnant. Thus, even if gravitational waves of a significant amplitude are not observed for the postmerger phase of binary neutron star mergers in the near-future gravitational-wave observation, we should not consider that such observation implies that a massive neutron star is not formed after the merger. On the other hand, if gravitational waves of a significant amplitude are observed for the postmerger phase of binary neutron star merger, we will be able to conclude that a massive neutron star is formed as a remnant and viscous effects do not play an important role for the merger remnant.

APPENDIX: CONVERGENCE AND ACCURACY

The results shown in this paper depend only weakly on the grid resolution. To demonstrate this fact, we plot the averaged angular velocity profile and gravitational waveforms in Fig. 6. This shows that the numerical results indeed depend very weakly on the grid resolutions. The plots of Fig. 6 show that our numerical results are reliable. This result illustrates a merit of employing viscous hydrodynamics, that we do not have to perform simulations with extremely high resolution in this framework, in contrast to the cases of MHD simulations.

To check the accuracy of our simulations, we also monitored the violation of the Hamiltonian constraint, denoted by $H = 0$. Following our previous paper [19], we focus on the following rest mass-averaged quantity,

$$\text{ERR} = \frac{1}{M_*} \int \rho_* \frac{|H|}{\sum_k |H_k|} d^3 x, \qquad (A1)$$

where $H = \sum_k H_k$ and H_k denotes individual components in H composed of the energy density, the square terms of the extrinsic curvature, and the three-dimensional Ricci scalar. M_* denotes the total rest mass of the system. ERR shows an averaged degree for the violation of the Hamiltonian constraint (for ERR = 0, the constraint is satisfied, while for ERR = 1, the Hamiltonian constraint is violated by 100%). Figure 7 plots the evolution of ERR for $\alpha_v = 0$ and 0.02 and for the three grid resolutions. As we showed in Ref. [19], the convergence with respect to the grid resolution is lost because the spatial derivative of the velocity, which presents in the equations of τ_{ij}, introduces a nonconvergent error. However, the degree of the violation is kept reasonably small, i.e., ERR $\lesssim 0.015$, in our simulation time, irrespective of the values of α_v. This approximately indicates that the Hamiltonian constraint is satisfied within a 1.5% error. Therefore, we conclude that the results obtained in this paper are reliable at least in our present simulation time.

[1] J. Abadie *et al.* (LIGO Scientific Collaboration), Nucl. Instrum. Methods Phys. Res., Sect. A **624**, 223 (2010): T. Accadia *et al.* Classical Quantum Gravity **28**, 025005 (2011); **28**, 079501(E) (2011); K. Kuroda, Classical Quantum Gravity **27**, 084004 (2010).

[2] P. B. Demorest, T. Pennucci, S. M. Ransom, M. S. E. Roberts, and J. W. T. Hessels, Nature (London) **467**, 1081 (2010); J. Antoniadis *et al.*, Science **340**, 1233232 (2013).

[3] M. Shibata, K. Taniguchi, and K. Uryū, Phys. Rev. D **71**, 084021 (2005): M. Shibata and K. Taniguchi, Phys. Rev. D **73**, 064027 (2006).

[4] K. Hotokezaka, K. Kyutoku, H. Okawa, M. Shibata, and K. Kiuchi, Phys. Rev. D **83**, 124008 (2011).

[5] A. Bauswein and H.-Th. Janka, Phys. Rev. Lett. **108**, 011101 (2012).

[6] K. Hotokezaka, K. Kiuchi, K. Kyutoku, T. Muranushi, Y.-I. Sekiguchi, M. Shibata, and K. Taniguchi, Phys. Rev. D **88**, 044026 (2013).

[7] K. Takami, L. Rezzolla, and L. Baiotti, Phys. Rev. D **91**, 064001 (2015).

[8] T. Dietrich, S. Bernuzzi, M. Ujevic, and B. Brügmann, Phys. Rev. D **91**, 124041 (2015).

[9] M. Shibata, *Numerical Relativity* (World Scientific, Singapore, 2016).

[10] L. Baiotti and L. Rezzolla, arXiv:1607.03540.

[11] D. J. Price and S. Rosswog, Science **312**, 719 (2006).

[12] K. Kiuchi, K. Kyutoku, Y. Sekiguchi, M. Shibata, and T. Wada, Phys. Rev. D **90**, 041502(R) (2014); K. Kiuchi, P. Cerda-Duran, K. Kyutoku, Y. Sekiguchi, and M. Shibata, Phys. Rev. D **92**, 124034 (2015).

[13] S. A. Balbus and J. F. Hawley, Rev. Mod. Phys. **70**, 1 (1998).

[14] J. F. Hawley, S. A. Richers, X. Guan, and J. H. Krolik, Astrophys. J. **772**, 102 (2013).

[15] T. K. Suzuki and S. Inutsuka, Astrophys. J. **784**, 121 (2014).

[16] J. M. Shi, J. M. Stone, and C. X. Huang, Mon. Not. R. Astron. Soc. **456**, 2273 (2016): G. Salvesen, J. B. Simon, P. J. Armitage, and M. C. Begelman, Mon. Not. R. Astron. Soc. **457**, 857 (2016).

[17] M. D. Duez, Y.-T. Liu, S. L. Shapiro, and B. C. Stephens, Phys. Rev. D **69**, 104030 (2004).

[18] D. Radice, Astrophys. J. Lett. **838**, L2 (2017).

[19] M. Shibata, K. Kiuchi, and Y. Sekiguchi, Phys. Rev. D **95**, 083005 (2017).

[20] W. Israel and J. M. Stewart, Ann. Phys. (N.Y.) **118**, 341 (1979).

[21] W. A. Hiscock and L. Lindblom, Ann. Phys. (N.Y.) **151**, 466 (1983).

[22] L. D. Landau and E. M. Lifshitz, *Fluid Mechanics* (Peragamon, London, 1959).

[23] N. I. Shakura and R. A. Sunyaev, Astron. Astrophys. **24**, 337 (1973): S. L. Shapiro and S. A. Teukolsky, *Black Holes, White Dwarfs, and Neutron Stars: The Physics of Compact Objects* (Wiley, New York, 1983), Chap. 14.

[24] M. Shibata and T. Nakamura, Phys. Rev. D **52**, 5428 (1995): T. W. Baumgarte and S. L. Shapiro, Phys. Rev. D **59**, 024007 (1998): M. Campanelli, C. O. Lousto, P. Marronetti, and Y. Zlochower, Phys. Rev. Lett. **96**, 111101 (2006): J. G. Baker, J. Centrella, D.-I. Choi, M. Koppitz, and J. van Meter, Phys. Rev. Lett. **96**, 111102 (2006).

[25] N. K. Glendenning and S. A. Moszkowski, Phys. Rev. Lett. **67**, 2414 (1991).

[26] J. S. Read, B. D. Lackey, B. J. Owen, and J. L. Friedman, Phys. Rev. D **79**, 124032 (2009).

[27] https://dcc.ligo.org/cgi-bin/DocDB/ShowDocument?docid=2974.